



**HAL**  
open science

# Replication-coupled histone H3.1 deposition determines nucleosome composition and heterochromatin dynamics during *Arabidopsis* seedling development

Matthias Benoit, Lauriane Simon, Sophie Desset, Céline Duc, Sylviane Cotterell, Axel Poulet, Samuel Le Goff, Christophe Tatout, Aline V Probst

## ► To cite this version:

Matthias Benoit, Lauriane Simon, Sophie Desset, Céline Duc, Sylviane Cotterell, et al.. Replication-coupled histone H3.1 deposition determines nucleosome composition and heterochromatin dynamics during *Arabidopsis* seedling development. *New Phytologist*, 2018, 221 (1), pp.385 - 398. 10.1111/nph.15248 . hal-04170933

**HAL Id: hal-04170933**

**<https://hal.inrae.fr/hal-04170933v1>**

Submitted on 25 Jul 2023

**HAL** is a multi-disciplinary open access archive for the deposit and dissemination of scientific research documents, whether they are published or not. The documents may come from teaching and research institutions in France or abroad, or from public or private research centers.

L'archive ouverte pluridisciplinaire **HAL**, est destinée au dépôt et à la diffusion de documents scientifiques de niveau recherche, publiés ou non, émanant des établissements d'enseignement et de recherche français ou étrangers, des laboratoires publics ou privés.

# Replication-coupled histone H3.1 deposition determines nucleosome composition and heterochromatin dynamics during *Arabidopsis* seedling development

Matthias Benoit<sup>1,2</sup> , Lauriane Simon<sup>1,3</sup>, Sophie Desset<sup>1</sup>, Céline Duc<sup>1</sup>, Sylviane Cotterell<sup>1</sup>, Axel Poulet<sup>1,4</sup>, Samuel Le Goff<sup>1</sup>, Christophe Tatout<sup>1</sup> and Aline V. Probst<sup>1</sup> 

<sup>1</sup>GREC, Université Clermont Auvergne, CNRS, INSERM, BP 38, 63001 Clermont-Ferrand, France; <sup>2</sup>The Sainsbury Laboratory, University of Cambridge, Cambridge CB2 1LR, UK;

<sup>3</sup>Department of Plant Biology, Uppsala BioCenter, Swedish University of Agricultural Sciences, Uppsala 75007, Sweden; <sup>4</sup>Department of Biostatistics and Bioinformatics, Rollins School of Public Health, Emory University, 1518 Clifton Road NE, Atlanta, GA 30322, USA

## Summary

Author for correspondence:

Aline V. Probst

Tel: +33 4 73 40 74 01

Email: [aline.probst@uca.fr](mailto:aline.probst@uca.fr)

Received: 30 January 2018

Accepted: 1 May 2018

*New Phytologist* (2019) **221**: 385–398

doi: 10.1111/nph.15248

**Key words:** *Arabidopsis thaliana*, CAF-1, chromatin, development, epigenetics, histone variant.

- Developmental phase transitions are often characterized by changes in the chromatin landscape and heterochromatin reorganization. In *Arabidopsis*, clustering of repetitive heterochromatic loci into so-called chromocenters is an important determinant of chromosome organization in nuclear space. Here, we investigated the molecular mechanisms involved in chromocenter formation during the switch from a heterotrophic to a photosynthetically competent state during early seedling development.
- We characterized the spatial organization and chromatin features at centromeric and pericentromeric repeats and identified mutant contexts with impaired chromocenter formation.
- We find that clustering of repetitive DNA loci into chromocenters takes place in a precise temporal window and results in reinforced transcriptional repression. Although repetitive sequences are enriched in H3K9me2 and linker histone H1 before repeat clustering, chromocenter formation involves increasing enrichment in H3.1 as well as H2A.W histone variants, hallmarks of heterochromatin. These processes are severely affected in mutants impaired in replication-coupled histone assembly mediated by CHROMATIN ASSEMBLY FACTOR 1 (CAF-1). We further reveal that histone deposition by CAF-1 is required for efficient H3K9me2 enrichment at repetitive sequences during chromocenter formation.
- Taken together, we show that chromocenter assembly during post-germination development requires dynamic changes in nucleosome composition and histone post-translational modifications orchestrated by the replication-coupled H3.1 deposition machinery.

## Introduction

Eukaryotic nuclear DNA is organized in chromatin. Different arrangements of arrays of nucleosomes, the basic subunits of chromatin, result in distinct higher-order chromatin structures within the nucleus. Although most active genes reside in open, transcription-permissive euchromatin, heterochromatin comprises mostly repetitive sequences and transposable elements that are transcriptionally silenced. Establishment and maintenance of heterochromatin is critical for chromosome segregation and genome integrity by preventing transcription and illegitimate recombination of repeated elements.

In certain yeast, animal and plant species, heterochromatin clusters in conspicuous, cytologically visible domains termed chromocenters (CCs). The formation of CCs is thought to contribute to heterochromatin stability by compartmentalizing repetitive elements and transposons away from euchromatin, and so

favoring concentration of chromatin silencing factors in specific subnuclear domains (Almouzni & Probst, 2011). Beyond its role in the transcriptional control of repetitive elements, nuclear organization of heterochromatin has a role in structuring the genome within the nuclear space. In *Arabidopsis thaliana*, CCs have been shown to contribute to the arrangement of chromosome territories by anchoring loops of gene-rich euchromatic domains (Fransz *et al.*, 2002; Feng *et al.*, 2014). Diploid *Arabidopsis* nuclei contain approximately six to 10 CCs mainly comprising clustered centromeric, pericentromeric and rDNA repeats, as well as transposable elements (Probst *et al.*, 2003; Simon *et al.*, 2015). These CCs are not randomly organized in the nucleus, but localize preferentially at the nuclear periphery (Fang & Spector, 2005; Poulet *et al.*, 2017). The number and distribution of CCs as well as the genetic elements forming a specific CC vary between cell-types and developmental stages with different gene expression programs (Mayer *et al.*, 2005; Fransz *et al.*, 2006; Benoit *et al.*,

2013), reflecting their role in organizing euchromatin in the nucleus. Furthermore, CCs are dynamically reorganized in response to developmental or environmental stimuli (Probst & Mittelsten Scheid, 2015). CCs transiently decondense in response to prolonged heat stress (Pecinka *et al.*, 2010), pathogen infection (Pavet *et al.*, 2006) or upon dedifferentiation into protoplasts (Tessadori *et al.*, 2007a), but are also dynamically rearranged during somatic-to-reproductive cell fate transitions in spore mother cells (She *et al.*, 2013; She & Baroux, 2015), in leaf tissue during developmental phase changes such as floral transition (Tessadori *et al.*, 2007b) or in cotyledons during photomorphogenesis (Bourbousse *et al.*, 2015; Snoek *et al.*, 2017) and germination (van Zanten *et al.*, 2011). In dry seeds, chromatin of cotyledon nuclei is highly condensed but a transient disruption of CCs occurs during seed imbibition, translating into dispersion of centromeric and pericentromeric repeats in the nuclear volume immediately after germination (van Zanten *et al.*, 2011). CC re-assembly then takes place in developing cotyledons between two and five days after germination (Mathieu *et al.*, 2003; Douet *et al.*, 2008). Dynamics of chromatin modifications occurring at repetitive sequences and molecular features driving CC re-assembly during this developmental window are poorly understood.

Repetitive elements forming CCs are enriched in repressive chromatin marks, including DNA methylation and histone post-translational modifications such as di-methylation of histone H3 Lys-9 (H3K9me2) and monomethylation of H3 Lys-27 (H3K27me1) (Probst *et al.*, 2003; Martens *et al.*, 2005; Mathieu *et al.*, 2005), which can form a binding platform for specific reader proteins. Heterochromatin further shows high nucleosomal density and low DNase I accessibility, landmarks of a compact chromatin state (Chodavarapu *et al.*, 2010; Shu *et al.*, 2012), possibly dampening its accessibility by transcription factors and the transcriptional machinery. In addition, through the incorporation of histone variants, biophysical features of the nucleosome can be modified with impacts on transcriptional competence and higher-order chromatin organization. For example, the histone H2A variant H2A.Z is a major regulator of gene transcription (Jin *et al.*, 2009; Thakar *et al.*, 2009; Sura *et al.*, 2017), whereas nucleosomes comprising the variant H2A.W are hallmarks of heterochromatin. Indeed, H2A.W has been shown *in vitro* to promote long-range chromatin fiber-to-fiber interactions through its conserved C-terminal tail and to increase higher-order chromatin condensation *in vivo* (Yelagandula *et al.*, 2014). Histone H3 variant H3.3 correlates with active gene expression (Stroud *et al.*, 2012; Wollmann *et al.*, 2012, 2017; Shu *et al.*, 2014; Duc *et al.*, 2017), its incorporation results in more unstable nucleosomes (Jin *et al.*, 2009; Thakar *et al.*, 2009) and a transcription-permissive chromatin state, whereas H3.1 is enriched at transcriptionally inactive chromatin (Stroud *et al.*, 2012; Wollmann *et al.*, 2012). Another feature of heterochromatin is the presence of linker histones H1 that bind to DNA both at the entry and exit site of the nucleosome particle and which are enriched at CCs (She *et al.*, 2013; Fyodorov *et al.*, 2018). Although the characteristics of heterochromatin in leaf tissues with conspicuous CCs were well defined in previous reports, few

studies have yet addressed the dynamic nature of CC structures and the implicated changes in chromatin features (Tessadori *et al.*, 2007a,b; van Zanten *et al.*, 2012; She *et al.*, 2013). To learn about the mechanisms involved in the formation of higher-order chromatin structures, we have taken advantage of the progressive formation of chromocenter structures that takes place during post-germination development and investigated the changes in histone variants and modifications in this dynamic system. We show that centromeric and pericentromeric repeats gather with similar dynamics into CC structures, a rearrangement that matches with consolidation of transcriptional repression of pericentromeric repeats during cotyledon post-germination development. We find that despite absence of most CCs early after germination, repetitive elements are already enriched in the heterochromatin-characteristic H3K9me2 mark and the linker histone H1. Instead, formation of CCs correlates with an increase in H3.1 and H2A.W variant occupancy that have the potential to modify nucleosome stability and chromatin fiber–fiber interaction, respectively. In agreement with increasing H3.1 occupancy, we find evidence that CHROMATIN ASSEMBLY FACTOR 1 (CAF-1)-mediated histone deposition, but not the replication-independent deposition mediated by the HISTONE REGULATOR (HIR) complex is required for proper CC formation. Loss of CAF-1 not only affects H3.1 and H2A.W enrichment, but also reduces H3K9me2 levels. We conclude that the CAF-1 mediated nucleosome assembly machinery coordinates nucleosomal occupancy and composition and contributes to the setting and propagation of post-translational modifications, ultimately influencing higher-order chromatin formation.

## Materials and Methods

### Plant material and growth conditions

Mutant *Arabidopsis thaliana* lines were obtained from the Nottingham Arabidopsis Stock Center (NASC) and/or have been kindly provided by other laboratories. Homozygous mutants *fas2-5* (SALK\_147693), a knock-out allele for the FAS2 subunit of the CAF-1 complex, *fas1-4* (SAIL-662-D10), a knock-down allele for the FAS1 subunit of the CAF-1 complex (Duc *et al.*, 2015), *hira-1* (WiscDsLox362H05), *htr9-1* (SALK\_148171), *h2a.w.6* (SALK\_024544.32) and *h2a.w.7* (GK\_149G05) are in the Columbia background and were identified by PCR-based genotyping. *h2a.w.6 h2a.w.7* double mutants were generated by crosses of single mutants. Transgenic plants expressing Myc-tagged H3.1 and H3.3 (Stroud *et al.*, 2012) were kindly provided by C. Gutierrez. Transgenic plants expressing H3.1 (HTR9) with a FLAG-HA tag, termed here epitope tagged H3.1 (eH3.1) under control of its endogenous promoter were described previously (Duc *et al.*, 2017). T<sub>3</sub> monolocus homozygous lines were crossed with *fas2-5* mutants to obtain eH3.1 *fas2-5* lines.

For *in vitro* culture, seeds were surface-sterilized and sown on germination media containing 0.8% w/v agar, 1% w/v sucrose and 1× Murashige & Skoog salts (MS, M0255; Duchefa Biochemie, Haarlem, Netherlands). After 2 d of stratification at 4°C in the dark, seedlings were grown under 16 h : 8 h, light : dark

cycles at 23°C. Cotyledons were harvested at 78, 102, 126 or 150 h after transfer to the growth chamber, corresponding to time points 2, 3, 4 or 5 d after germination (dag), respectively.

### RNA extraction and RT-qPCR

Total RNAs were extracted from dissected and shock-frozen cotyledons using Tri-Reagent (Euromedex, Souffelweyersheim, France), treated with RQ1 DNase I (Promega, Madison, WI, USA) and purified with Phenol-Chloroform. Reverse transcription was primed either with oligo(dT)15 or random hexamers supplemented with reverse primers for *TSI* and *Ta3* using M-MLV reverse transcriptase (Promega). Transcript levels were determined by quantitative polymerase chain reaction (qPCR) with the LightCycler<sup>®</sup> 480 SYBR Green I Master kit (Roche, Basel, Switzerland) (Roche, Basel, Switzerland) on the Roche LightCycler<sup>®</sup> 480 and normalized to *MON1* (*At2g28390*) transcript levels (Czechowski *et al.*, 2005), using the comparative threshold cycle method.

### 3D-quantification of nuclear parameters

Col-0 wild type (WT) seedlings were harvested 78 h and 150 h after transfer of the seeds to the growth chamber. In brief, cotyledons were collected and fixed using 1% formaldehyde and 10% DMSO in 1 × PBS with 6.7 mM EGTA (pH 7.5) under vacuum for 5 min and incubated for 25 min at room temperature (Desset *et al.*, 2018). Tissues were then washed with methanol and ethanol to obtain transparent tissue preparations. After rehydration, fixed tissues were stained overnight at 4°C in a solution of Hoechst 33258 (Sigma, St Louis, MO, USA) at 0.25 µg ml<sup>-1</sup> in PBS. Stained cotyledons were placed on a slide in PBS: glycerol (20:80) solution and covered with a coverslip for microscopic observations using structured illumination microscopy to produce confocal-like images using an Optigrid module (Leica Microsystems MAAF DM 16000B) with a ×63 oil objective. The IMAGEJ plugin NUCLEUSJ was used to characterize nuclear morphology and chromatin organization (Poulet *et al.*, 2015).

### Fluorescence *in situ* hybridization

For fluorescence *in situ* hybridization (FISH), *in vitro*-grown cotyledons aged from 2 to 5 dag were fixed in ethanol-acetic acid (3:1 v/v) and FISH was performed as described (Bowler *et al.*, 2004). Slides were analyzed with a Zeiss Axio Imager Z.1 microscope equipped with a Zeiss AxioCam MRm camera system and images processed with IMAGEJ and Adobe PHOTOSHOP. More than 200 nuclei were scored per condition using a double-blind experimental setup. Only nuclei in which all 180-bp and *Transcriptionally Silent Information (TSI)* repeats are clustered in CCs are scored as 'clustered'.

### Protein immunolocalization

For immunofluorescence assays, dissected cotyledons were fixed in 4% formaldehyde (Sigma) in Tris buffer, finely chopped in

Lysis Buffer (15 mM Tris-HCl pH 7.5, 80 mM KCl, 2 mM EDTA, 0.5 mM spermidine, 0.5 mM spermine, 20 mM NaCl, 0.1% Triton X-100) and the homogenate filtered through a 30-µm filter before centrifugation. The nuclei pellet was resuspended in sorting buffer (100 mM Tris-HCl pH 7.5, 50 mM KCl, 2 mM MgCl<sub>2</sub>, 0.05% Tween 20 and 5% sucrose) and deposited onto a microscope slide before air-drying. Nuclei preparations were fixed in 2% formaldehyde in PBS, washed with water and air-dried. Slides were incubated with the anti-HA antibody (Abcam, Cambridge, UK; batch GR218331-6) overnight, and the primary antibody was revealed with a secondary anti-rabbit antibody coupled to Alexa-488 (Molecular Probes, Eugene, OR, USA). Slides were mounted in Vectashield (Vector Laboratories, Peterborough, UK) with 4',6-diamidino-2-phenylindole (DAPI) (2 µg ml<sup>-1</sup>). For microscopic observation, a fluorescence light microscope DM6000B (Leica, Wetzlar, Germany) with a digital CMOS ORCA – Flash4.0 camera (Hamamatsu, Hamamatsu City, Japan) was used.

### Chromatin immunoprecipitation

Chromatin was isolated from cotyledons as described (Bowler *et al.*, 2004) after formaldehyde cross-linking. Chromatin was sheared using a Diagenode Bioruptor (10 cycles, 30 s ON, 90 s OFF). Chromatin immunoprecipitation (ChIP) was carried out with the LowCell# ChIP kit (Diagenode, Seraing, Belgium) followed by qPCR quantification. For each ChIP shown in Figs 4 and 5 (see later), WT and *fas2-5* samples at 2 and 5 dag were processed together. To adjust for different IP efficiencies between the independent ChIP experiments, IP levels normalized to input (for H3, H2A.W and H1) or H3 (for H3K9me2) were set to 1 for *Ta3* in the Col-0 2-dag sample. Anti-H3 (ab1791, Abcam, batches GR242835-1, GR265016-1 and GR172700-1), anti-H3K9me2 (ab1220, Abcam, batch GR166768-3), anti-H2A.W.6 (Yelagandula *et al.*, 2014), kindly provided by Z. Lorkovic and F. Berger), anti-H1 (AS11 801, Agrisera, Vänäs, Sweden; batch 1512), anti-Myc (05-724, Millipore, Burlington, MA, USA; batch 2720363) and FLAG-coupled magnetic beads (M8823, Sigma, batch SBL1128V) were used.

### Primers

All primer sequences are listed in Supporting Information Table S1.

### Statistical analysis

A two-sided Student's *t*-test was used for mean comparison for FISH analyses, transcript levels and local enrichments determined by ChIP-qPCR. Asterisks in the figures indicate statistically significant differences (•,  $P < 0.1$ ; \*\*,  $P < 0.05$ ; \*\*\*,  $P < 0.01$ ; \*\*\*\*,  $P < 0.001$ ). Hashtags denote statistically significant differences between WT and *fas2-5* at the same time point (#,  $P < 0.1$ ; ##,  $P < 0.05$ ). Statistical significance for nuclear morphometric parameters determined with NUCLEUSJ was determined using a nonparametric Kruskal–Wallis test (\*,  $P < 0.05$ ; \*\*,  $P < 0.01$ ;

\*\*\*,  $P < 0.001$ ). Hashtags denote statistically significant differences between WT and *fas2-5* at the same time point (###,  $P < 0.001$ ).

## Results

### Progressive formation of CCs during postgermination development is associated with transcriptional repression

The first days of postgermination development involve important rearrangements of nuclear architecture (Mathieu *et al.*, 2003; Douet *et al.*, 2008). To gain a global view of the changes in nuclear features and chromatin organization during this developmental time window, we fixed cotyledons from seedlings at 2 and 5 dag, acquired 3D-images of epidermis nuclei after DNA staining with Hoechst (Fig. 1a) and measured parameters relative to nuclear morphology and CC organization. We find that nuclei change their shape during this developmental time window, nuclei at 5 dag being more elongated than those at 2 dag (Fig. 1b). As CCs are highly condensed chromatin domains that stain intensively with DNA-intercalating agents, they can be segmented from the lightly stained euchromatic regions and their characteristics quantified (Poulet *et al.*, 2015). Between 2 and 5 dag, the median CC number increased significantly from six to eight CCs and the total CC volume increased significantly from a median volume of 3.3 to 4.4  $\mu\text{m}^3$  resulting in an elevated relative heterochromatin volume (RHV) of the nuclei at 5 dag (Fig. 1b). Together, this suggests gradual changes in the organization of repetitive sequences that form CCs.

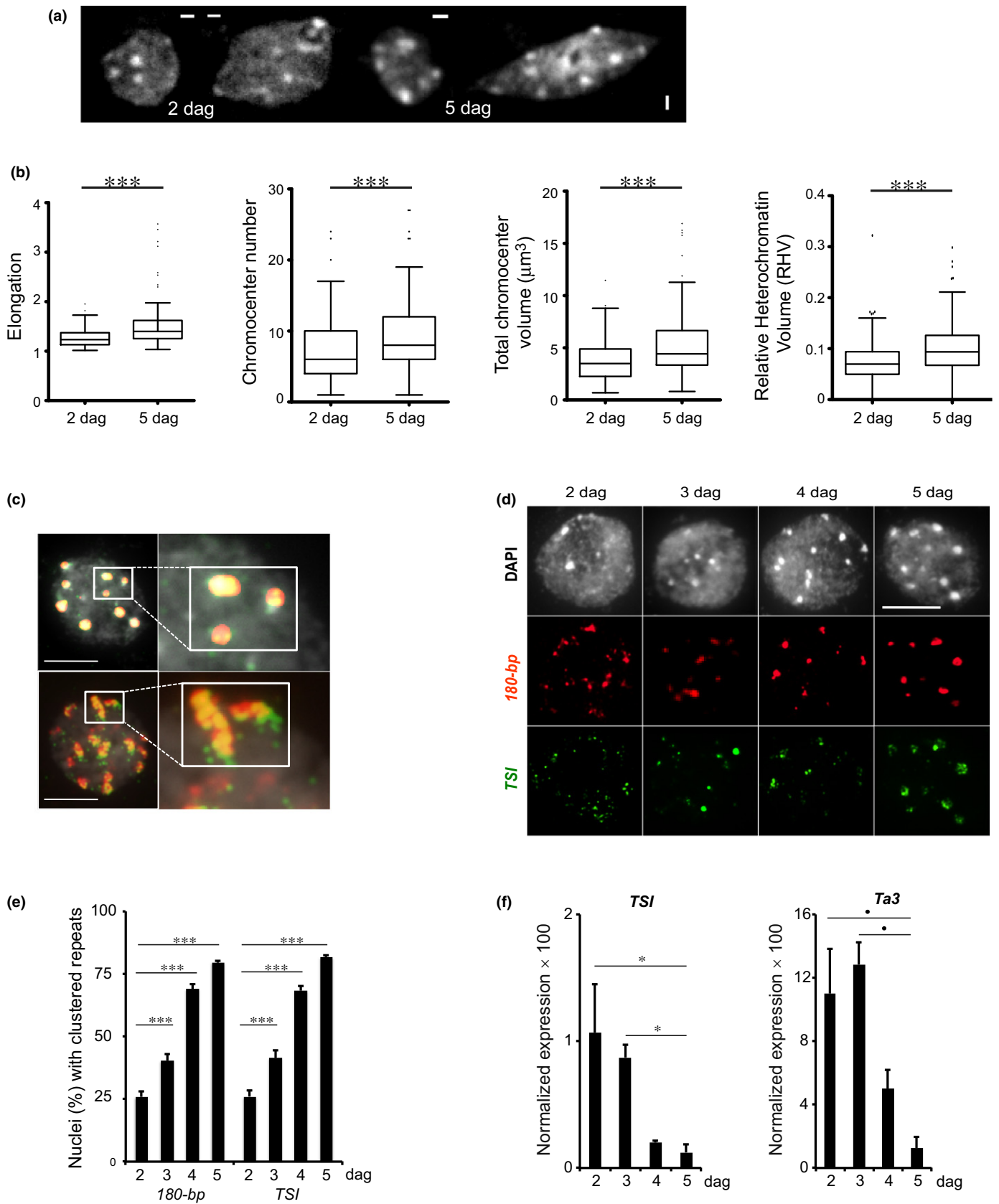
In order to get a higher resolution view on the organization of specific repetitive sequences in the nucleus, we performed FISH targeting centromeric (180-bp) and pericentromeric (*TSI*) repeats present on all chromosomes (Probst *et al.*, 2003). We quantified the organization of heterochromatic repeats into CCs by assessing the percentage of nuclei with fully clustered FISH signals (Fig. 1c,e). At 2 dag, cotyledon nuclei exhibit small heterochromatic foci, visible by DAPI staining, which we refer to as 'pre-CCs', and only *c.* 25% of the nuclei reveal completely clustered repeats compared to *c.* 80% at 5 dag (Fig. 1d,e). The analyzed centromeric and pericentromeric sequences cluster into CCs with a precise temporal arrangement and with similar dynamics. Centromeric and pericentromeric repeats, as well as most transposable elements are transcriptionally silent (Steimer *et al.*, 2000; May *et al.*, 2005). To test whether the different arrangement of

repetitive sequences influences their transcription, we quantified transcript levels of *TSI* repeats and the pericentromeric *Ta3* retrotransposon (Konieczny *et al.*, 1991) by RT-qPCR using total RNA isolated from dissected cotyledons. We reproducibly observed approximately four-fold higher transcript levels of *TSI* and *Ta3* transcripts in cotyledons 2 dag, when these genomic regions are dispersed in 75% of the nuclei (Fig. 1f), compared to 5 dag. We conclude that heterochromatic repeats progressively cluster into CCs between 2 to 5 dag and that CC formation correlates with reduced levels of *TSI* and *Ta3* transcripts.

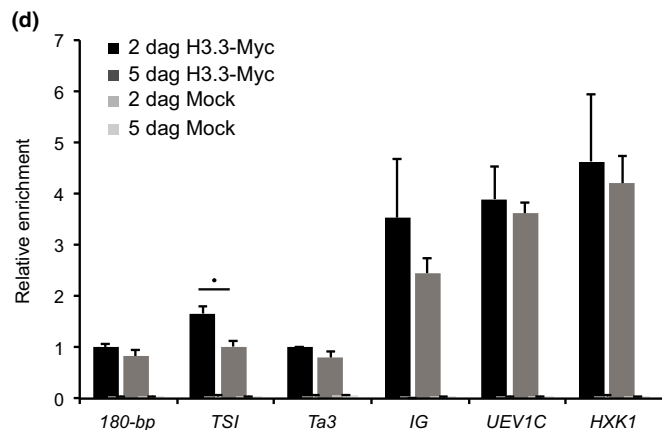
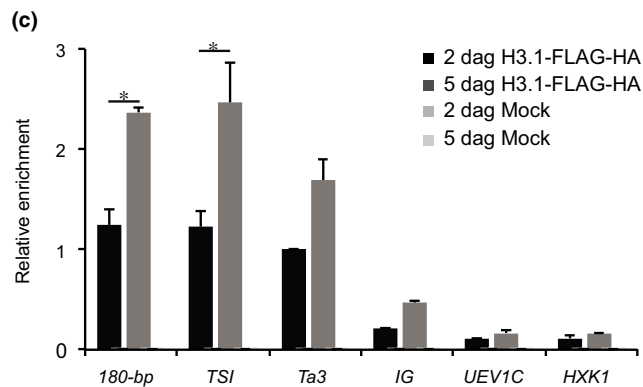
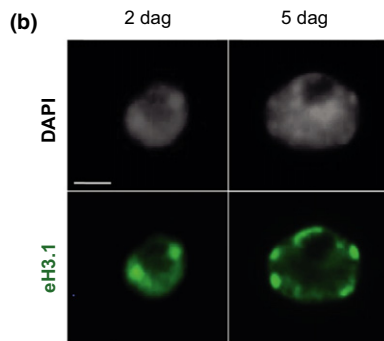
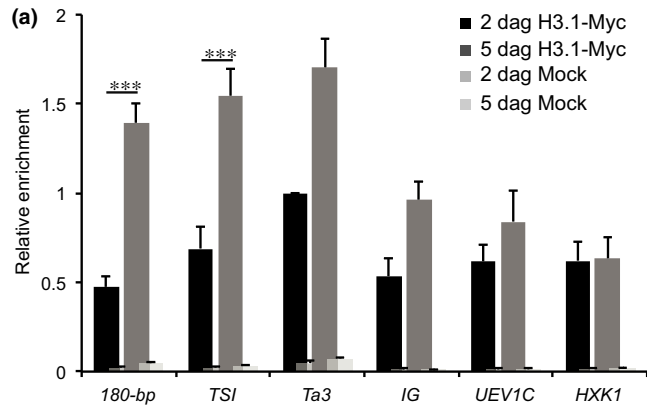
### H3.1 occupancy increases at repetitive sequences during CC formation

In order to gain further insight into changes of local chromatin features during CC formation at these repetitive elements, we explored histone dynamics and nucleosome composition. The first step in nucleosome assembly is the deposition of the H3–H4 tetramer (Smith & Stillman, 1991). We therefore investigated nucleosome composition in the replicative histone H3.1 and the replacement variant H3.3 using ChIP. H3.1 and H3.3 differ by only four amino acids and no discriminant antibody is available in plants. Hence, we used plant lines expressing translational fusions of H3.1 (HISTONE THREE RELATED 13; HTR13) and H3.3 (HTR5) with a Myc-tag (Stroud *et al.*, 2012) to specifically immuno-precipitate either H3.1 or H3.3. We noticed dynamic variations in H3.1 enrichment, with an increase in H3.1 occupancy at centromeric 180-bp repeats, pericentromeric sequences *TSI* and *Ta3* at 5 dag compared to 2 dag (Fig. 2a). The observed H3.1 enrichment cannot be explained by higher *H3.1* transcript levels, because those are lower at 5 dag than at 2 dag (Fig. S1a). To test H3.1 occupancy dynamics of another independent H3.1 gene product and to take into account potential changes in total H3.1 levels in the H3.1-Myc tagged lines, we used a transgenic epitope tagged H3.1 (eH3.1) line expressing the *HTR9* coding sequence fused to a short FLAG-HA epitope under control of the endogenous promoter in a *htr9* mutant background (Duc *et al.*, 2017). Immunofluorescence staining of cotyledon nuclei showed that HTR9-FLAG-HA is first enriched at the few visible conspicuous 'pre-CC' structures at 2 dag and then in all mature CCs at 5 dag (Fig. 2b). Quantification by anti-FLAG ChIP (Fig. 2c) revealed higher H3.1 occupancy at 5 dag compared to 2 dag at heterochromatic regions, whereas it remained low at two genes with different expression levels

**Fig. 1** Gradual clustering of repetitive elements into chromocenters correlates with reinforcement of transcriptional silencing. (a) Representative wild-type (WT) *Arabidopsis thaliana* cotyledon epidermis nuclei at 2 and 5 d after germination (dag) stained with Hoechst. (b) Quantification of nuclear elongation, chromocenter (CC) number, total CC volume per nucleus and the relative heterochromatin volume (RHV) in WT cotyledon nuclei at 2 and 5 dag as determined with NUCLEUSJ. The box represents the 25–75<sup>th</sup> percentiles, and the median is indicated. The whiskers are equal to 1.5× the interquartile range. Outliers are represented by dots; 2 dag,  $n = 133$ ; 5 dag,  $n = 134$ . \*,  $P < 0.05$ ; \*\*\*,  $P < 0.001$  (Kruskal–Wallis nonparametric test). (c, d) Representative nuclei submitted to DNA fluorescence *in situ* hybridization (FISH) with probes for 180-bp (red) and *Transcriptionally Silent Information* (*TSI*) (green) sequences and counterstained with 4',6-diamidino-2-phenylindole (DAPI) (grey). (c) Example of a clustered (top) and dispersed (bottom) organization of centromeric and pericentromeric sequences. (d) Representative nuclei from cotyledons aged 2, 3, 4 or 5 dag. (e) Percentage of nuclei ( $\pm$  SEM from seven biological replicates) with complete clustering of 180-bp or *TSI* repeats in CCs,  $n > 700$ . \*\*\*,  $P < 0.001$  (Student's *t*-test). (f) Reverse transcription polymerase chain reaction analysis of *TSI* (left) and *Ta3* (right) transcript levels in WT cotyledons at 2, 3, 4 and 5 dag. Histograms show normalized expression  $\pm$  SEM from at least two biological replicates. •,  $P < 0.1$ ; \*,  $P < 0.05$  (Student's *t*-test). Bars: (a) 1  $\mu\text{m}$ ; (c, d) 5  $\mu\text{m}$ .



(*UEVIC* and *HXK1*; Duc *et al.*, 2015) and at an intergenic region. This showed a strong differential enrichment in H3.1 between heterochromatin and euchromatin in nuclei of 5 dag



cotyledons. By contrast, H3.3 occupancy is high at active genes and low at heterochromatin already at 2 dag, remaining globally unchanged during this time window with only modest reduction at *TSI* repeats by 5 dag (Fig. 2d).

Together, these observations reveal that centromeric and pericentromeric repeats have a specific nucleosomal composition during early seedling development, with lower H3.1 occupancy in cotyledon nuclei early after germination compared to 5 dag. In agreement, data mining of recent transcriptomics data (Kawakatsu *et al.*, 2017) revealed low to undetectable transcript levels of most *H3.1*-encoding genes in dry seeds and re-expression during germination (Fig. S1b). The increasing H3.1 levels observed at centromeric and pericentromeric repeats during CC formation suggests a role for H3.1 deposition in the establishment of CCs as specialized chromatin domains.

### Chromatin assembly mediated by CAF-1 is required for CC formation

H3.1 is deposited by the CAF-1 complex that operates in a DNA-synthesis dependent manner (Otero *et al.*, 2016; Jiang & Berger, 2017), whereas the HIR complex is responsible for assembly of the replacement variant H3.3 (Nie *et al.*, 2014; Duc *et al.*, 2015). *FASCIATA 1* (*FAS1*), *FASCIATA 2* (*FAS2*) and *HISTONE REGULATOR A* (*HIRA*), encoding two subunits of the Arabidopsis CAF-1 complex, and the central subunit of the HIR complex, respectively, are expressed during early post-germination development in cotyledons (Fig. S2a). *FAS1* transcript levels are approximately seven-fold lower at 5 dag compared to 2 dag following the pattern of *H3.1* encoding genes (Fig. S2a), corroborating previous observations obtained using a *ProFAS1::GUS* reporter gene (Ramirez-Parra & Gutierrez, 2007). Arabidopsis mutants lacking functional CAF-1 and HIR complexes are viable (Kaya *et al.*, 2001; Nie *et al.*, 2014; Duc *et al.*, 2015) allowing us to test whether CC dynamics are altered in the respective histone chaperone mutant backgrounds. We first confirmed that loss of CAF-1 impacts H3.1 incorporation in our lines. Indeed, when the eH3.1 locus was introgressed into *fas2-5*

**Fig. 2** Dynamic H3.1 occupancy at repetitive sequences during chromocenter formation. (a) H3.1 (HTR13-Myc) occupancy determined by Myc-ChIP-qPCR relative to input at 180-bp centromeric repeats, pericentromeric repeats *Transcriptionally Silent Information* (*TSI*), the retrotransposon *Ta3*, an intergenic region (*IG*) and two genes (*UEVIC* and *HXK1*) in *Arabidopsis thaliana* cotyledons at 2 and 5 d after germination (dag). (b) Subnuclear localization of HTR9-FLAG-HA (eH3.1) revealed by immunostaining (green) in nuclei of cotyledons aged 2 or 5 dag. DNA is counterstained with 4',6-diamidino-2-phenylindole (DAPI) (grey). Bar, 5  $\mu$ m. (c) H3.1 occupancy determined by FLAG-ChIP-qPCR relative to input in cotyledons from wild-type (WT) plants aged 2 or 5 dag at the same targets as in (a). (d) H3.3 (HTR5-Myc) occupancy as determined by Myc-ChIP-qPCR relative to input in cotyledons from WT plants aged 2 or 5 dag at the same targets as in (a). Histograms in (a, c, d) show mean percentage  $\pm$  SEM relative to input for two or three biological replicates and occupancy at *Ta3* in each chromatin immunoprecipitation (ChIP) was set to 1. Each panel includes the no-antibody fraction (Mock) for comparison (light colors), which is shown to scale and might be hardly visible in some panels. •,  $P < 0.1$ ; \*,  $P < 0.05$ ; \*\*\*,  $P < 0.001$  (Student's *t*-test).

mutants to specifically follow H3.1 loading, we detected reduced H3.1 incorporation in *fas2-5* mutant plantlets by Western blot analysis of nuclear histones (Fig. S2b–d; Methods S1). We then quantified the clustering of centromeric and pericentromeric repeats by FISH in *fas1-4*, *fas2-5* and *hira-1* mutant plants

(Figs 3a,b, S2e,f). At 4 dag, significantly fewer (*c.* 45% in *fas2-5* vs *c.* 70% in WT) nuclei with completely clustered centromeric and pericentromeric repeats can be observed and only *c.* 55% of the *fas2-5* mutant nuclei compared to *c.* 80% in WT reach an organization in which all repeats are clustered in CCs at 5 dag (Fig. 3b). Altered CC formation was confirmed in *fas1-4* mutants, whereas loss of HIRA did not negatively affect CC formation (Fig. S2e,f). 3D analysis of cotyledon nuclei stained with Hoechst further revealed a reduced total volume of CCs and a reduced RHV in *fas2-5* mutants relative to the respective WT developmental stage (Fig. 3c). Furthermore, the total CC volume and the RHV did not increase significantly between 2 and 5 dag in the mutant context, confirming that the dynamics of CC reorganization are affected. The number of CCs rose between 2 and 5 dag in *fas2-5*, but even fewer CCs could be detected at 2 dag compared to WT (Fig. 3c).

Taken together, although HIRA-mediated replacement histone deposition does not impair clustering of repetitive elements into CCs, loss of CAF-1 function affects CC formation, suggesting a primary role for H3.1 incorporation in heterochromatin organization in cotyledons.

### Linker histone H1 and H2A.W enrichment during CC formation

We hypothesized that impaired nucleosome assembly coupled to DNA replication could impact nucleosome occupancy, nucleosome composition and ultimately CC formation. We therefore first analyzed whether deficient H3.1 incorporation in *fas2-5* mutants might be compensated by higher *H3.3* expression. Although transcript levels of the H3.3-encoding genes *HTR5* and *HTR8* are only moderately increased in CAF-1 mutants, the H3.3-like genes *HTR14* and in particular *HTR6* are expressed to *c.* two-fold and *c.* 70-fold higher levels, respectively, in the *fas2-5* mutant at 2 dag (Fig. S3a,b). Again, this could promote differential nucleosome composition in *fas2-5* mutants compared to WT. We then assessed H3 occupancy by H3-ChIP at 2 and 5 dag in WT and *fas2-5* mutant plants. Albeit this analysis does not differentiate between the diverse H3 variants, we found a small, but

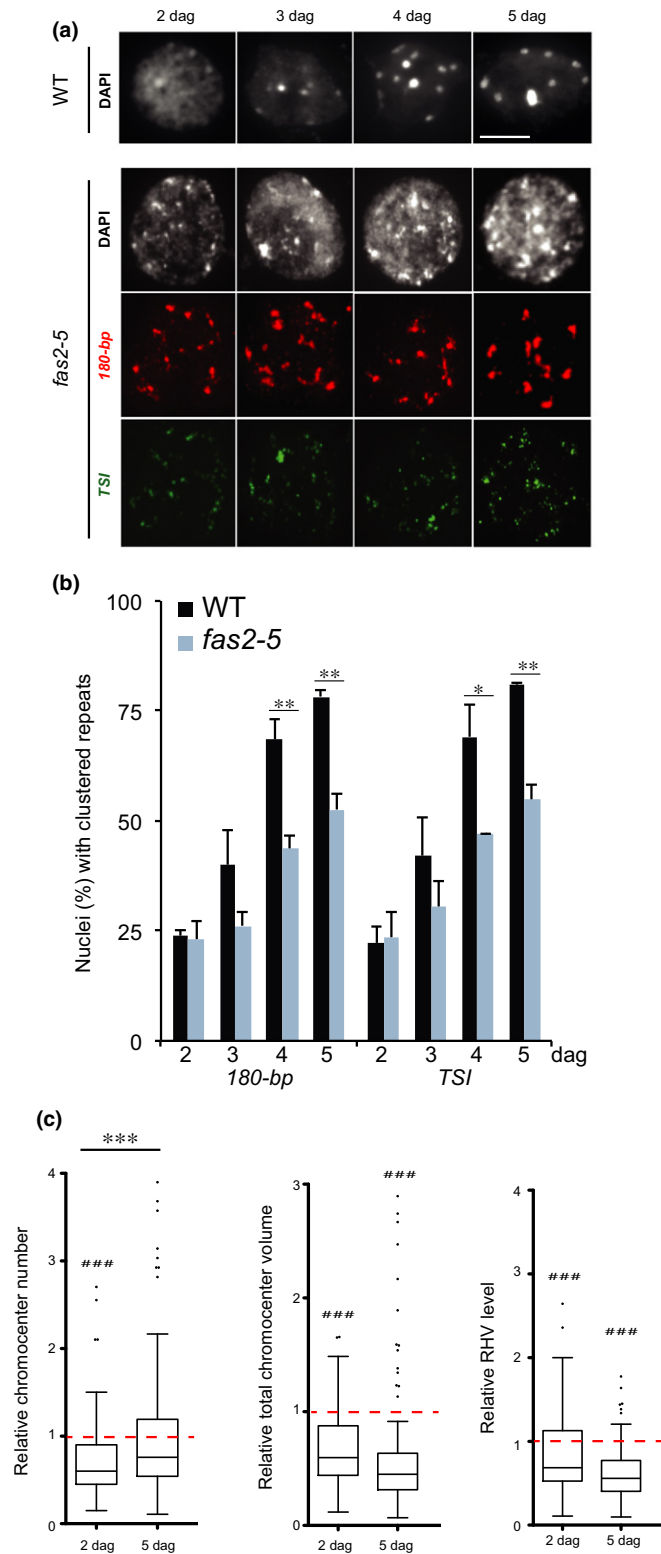


**Fig. 3** CHROMATIN ASSEMBLY FACTOR 1 (CAF-1) is required for chromocenter formation. (a) Representative nuclei from wild-type (WT) and *fas2-5* mutant *Arabidopsis thaliana* cotyledons stained with 4',6-diamidino-2-phenylindole (DAPI) (grey). For *fas2-5* mutant nuclei distribution of 180-bp (red) and Transcriptionally Silent Information (TSI) (green) sequences revealed by DNA fluorescence *in situ* hybridization (FISH) is shown. Bar, 5  $\mu$ m. (b) Percentage of nuclei ( $\pm$  SEM from two biological replicates) in WT and *fas2-5* mutants with complete clustering of 180-bp and TSI repeats in chromocenters (CCs),  $n > 200$ . \*,  $P < 0.05$ ; \*\*,  $P < 0.01$  (Student's *t*-test). (c) Boxplots showing total CC number, total CC volume per nucleus and the relative heterochromatin volume (RHV) in *fas2-5* mutants standardized using the WT mean set as 1 (red dashed line) for the corresponding developmental stage. The box represents the 25–75<sup>th</sup> percentiles, and the median is indicated. The whiskers are equal to 1.5 $\times$  the interquartile range. Outliers are represented by dots. Two days after germination (dag) vs 5 dag in *fas2-5*: \*\*\*,  $P < 0.001$ ; WT vs *fas2-5* at the corresponding dag: ###,  $P < 0.001$  (nonparametric Kruskal–Wallis test); 2 dag,  $n = 114$ ; 5 dag,  $n = 106$ .



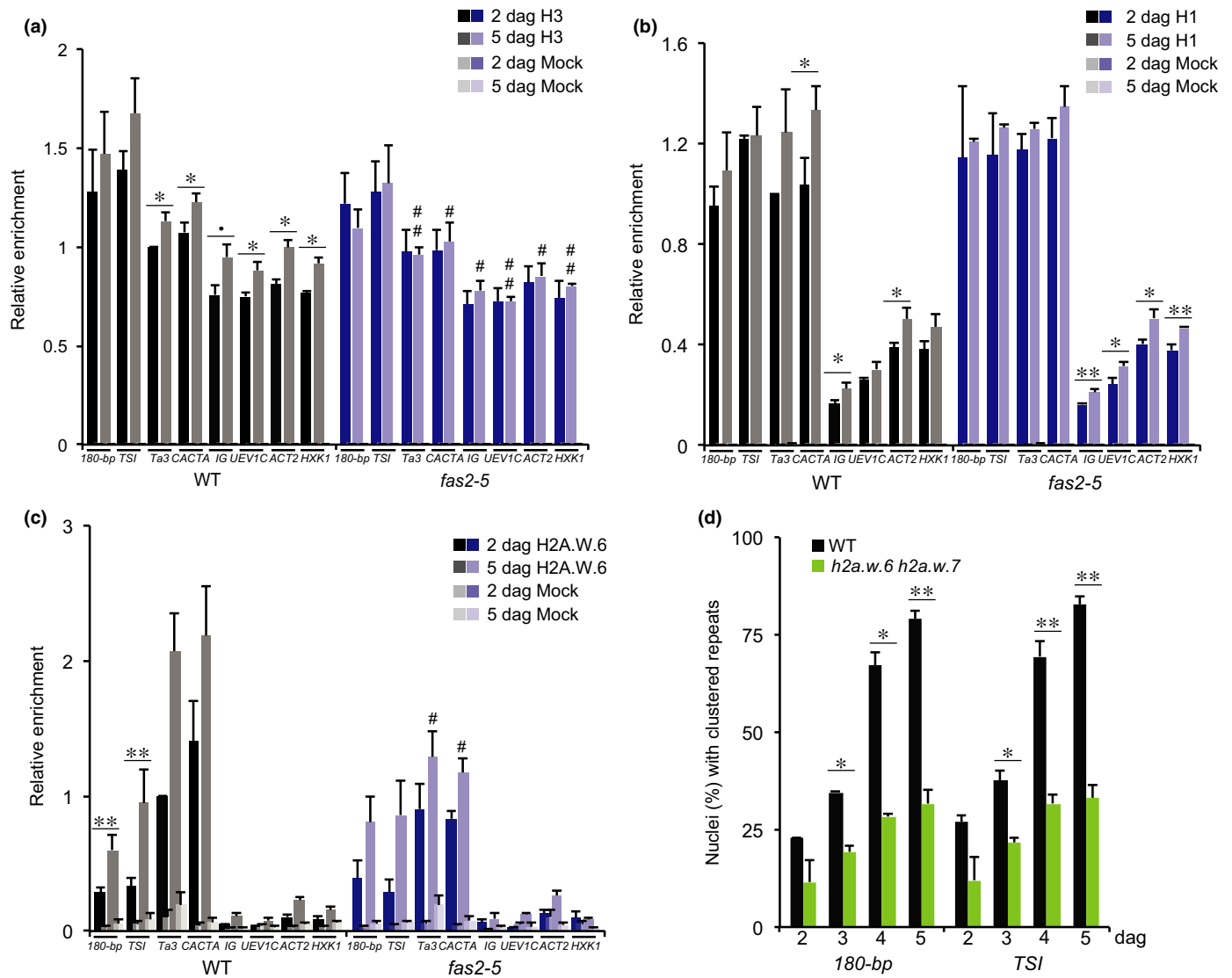


**Fig. 4** Loss of CHROMATIN ASSEMBLY FACTOR 1 (CAF-1) correlates with reduced H3 occupancy and affects H2A.W.6 enrichment at transposons. (a) H3, (b) H1 and (c) H2A.W.6 occupancy in wild-type (WT) and *fas2-5* mutant *Arabidopsis thaliana* cotyledons at 180-bp, *Transcriptionally Silent Information (TSI)*, *Ta3* and *CACTA*, three genes (*UEV1C*, *ACT2* and *HXK1*) and an intergenic region (*IG*) at 2 and 5 d after germination (dag) as determined by chromatin immunoprecipitation (ChIP)-quantitative polymerase chain reaction (qPCR). Histograms present mean percentages  $\pm$  SE for at least three biological replicates. Enrichment at *Ta3* at 2 dag in WT was set to 1. 2 dag vs 5 dag WT: \*,  $P < 0.1$ ; \*\*,  $P < 0.05$ ; \*\*\*,  $P < 0.01$ . WT vs *fas2-5* at the corresponding dag: #,  $P < 0.1$ ; ##,  $P < 0.05$  (Student's *t*-test). Each panel includes the no-antibody fraction (Mock) for comparison (light colors), which is shown to scale and might be hardly visible in some panels. (d) Percentage of nuclei ( $\pm$  SEM from two biological replicates) in WT and *h2a.w.6 h2a.w.7* double mutants with complete clustering of 180-bp and TSI repeats in chromocenters (CCs),  $n > 200$ . \*,  $P < 0.05$ ; \*\*,  $P < 0.01$  (Student's *t*-test).

consistent increase in H3 occupancy between 2 and 5 dag in WT plants, which is lost in *fas2-5* mutant cotyledons (Fig. 4a).

Linker histones have been associated with condensed chromatin and are suggested to stabilize higher-order chromatin structures (Fyodorov *et al.*, 2018). To explore a possible role for H1 in CC formation, we investigated the distribution of H1 using a commercially available H1 antibody (She *et al.*, 2013). We first confirmed that the resulting enrichment profile reflects the one obtained by immunoprecipitating a green fluorescent protein (GFP)-tagged H1.1 protein (She *et al.*, 2013) (Fig. S3c) and then assessed endogenous H1 occupancy in WT and *fas2-5* mutant cotyledons using the anti-H1 antibody. H1 occupancy is higher in heterochromatin than in euchromatin at 2 dag and

5 dag in WT, as expected (Rutowicz *et al.*, 2015), and this was also the case in *fas2-5* mutant cotyledons. Moreover, H1 occupancy varies only marginally during CC formation or in absence of replication-coupled histone assembly (Fig. 4b).

Next, we investigated the distribution of the histone variant H2A.W using an antibody directed against the H2A.W.6 protein encoded by *HTA6*, the most highly expressed H2A.W encoding gene in Arabidopsis (Fig. S3d) (Yelagandula *et al.*, 2014). Interestingly, H2A.W.6 occupancy increases during CC formation, H2A.W.6 enrichment at repetitive sequences being *c.* two-fold higher at 5 dag compared to 2 dag (Fig. 4c). Given the ability of H2A.W to promote chromatin fiber–fiber interactions, this suggests that deposition of H2A.W.6 during this developmental

time window contributes to the clustering of repetitive sequences into CCs. To test this hypothesis, we used *h2a.w.6 h2a.w.7* double mutants to assess CC formation in cotyledons with reduced H2A.W content. Clustering of 180-bp as well as TSI sequences is significantly impaired in plants with reduced H2A.W occupancy (Fig. 4d), confirming an important role for H2A.W deposition in CC formation (Yelagandula *et al.*, 2014). We then analyzed whether deficient H3.1 deposition in *fas2-5* mutants would affect H2A.W.6 occupancy. In *fas2-5* mutant cotyledons, H2A.W.6 occupancy is significantly reduced at *Ta3* and the *CACTA* transposon situated in the heterochromatic knob on chromosome 4,

in agreement with lower nucleosomal occupancy observed at these transposable elements (Fig. 4a,c).

Taken together, the presence of H1 precedes clustering of centromeric and pericentromeric sequences into CC structures and H1 deposition seems to be unaffected in plants lacking CAF-1. Instead, incorporation of H2A.W contributes to CC formation and is impaired in the absence of CAF-1.

### Deficient replication-coupled H3.1 deposition affects H3K9me2 enrichment

Centromeric and pericentromeric repetitive sequences are highly di-methylated at H3K9 and H3K9me2 distribution globally correlates with H3.1 occupancy (Stroud *et al.*, 2012; Wollmann *et al.*, 2012). Furthermore, in mammals, H3.1 is preferentially enriched in H3K9me3 compared to H3.3 (Loyola *et al.*, 2006), leaving the possibility that H3K9me2 might also be differentially enriched on H3.1 and H3.3 in plants. We therefore probed whether deficient H3.1 deposition may affect H3K9me2 levels during CC formation. ChIP analysis with a H3K9me2-specific antibody in WT and *fas2-5* mutants revealed that repetitive sequences are strongly enriched in H3K9me2 as early as 2 dag compared to the intergenic or genic regions tested and no further enrichment is observed at 5 dag when CCs are completely formed (Fig. 5a). The H3K9me2 mark is therefore set before CC formation. In *fas2-5* mutants, we reproducibly find 1.5 to two-fold less H3K9me2 at 2 and at 5 dag compared to the corresponding time points in WT plants (Fig. 5a), indicating that replication-coupled nucleosome assembly is required for efficient H3K9 di-

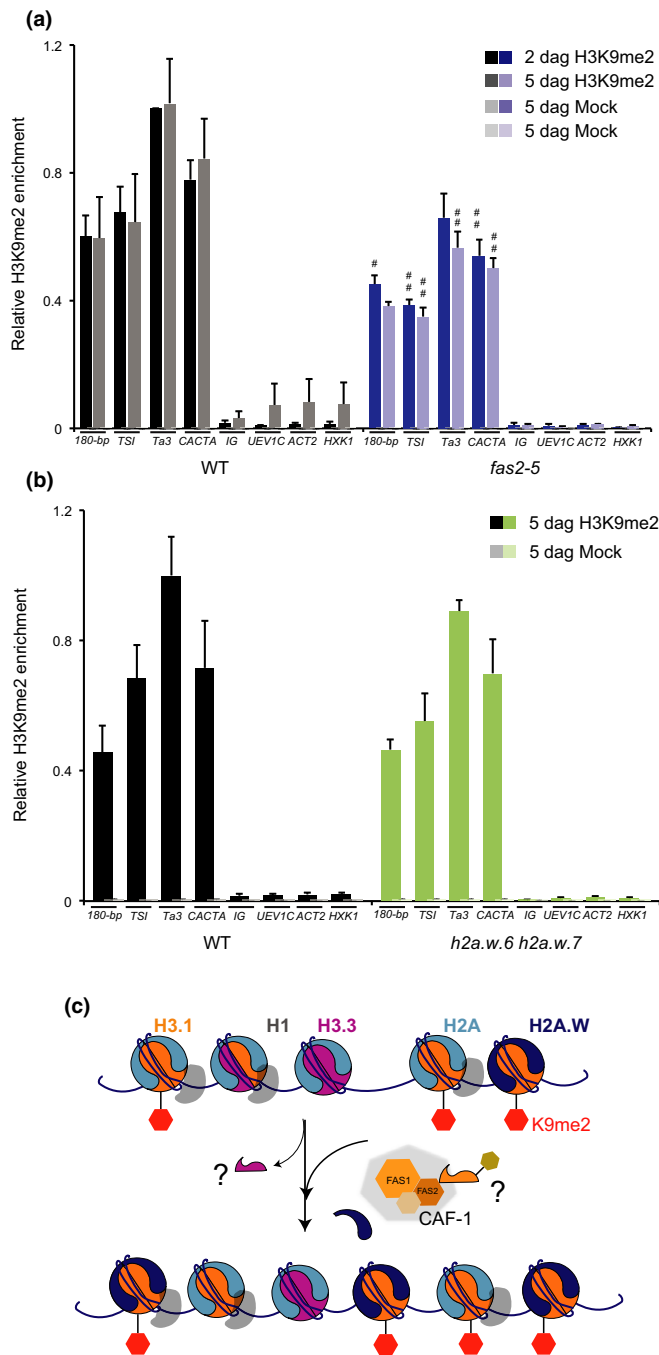


**Fig. 5** CHROMATIN ASSEMBLY FACTOR 1 (CAF-1) is required for H3K9me2 deposition at heterochromatic repeats. (a) H3K9me2 enrichment in wild type (WT) and *fas2-5 Arabidopsis thaliana* mutants relative to H3 occupancy at 180-bp, *Transcriptionally Silent Information (TSI)*, *Ta3* and *CACTA*, three genes (*UEV1C*, *ACT2* and *HXX1*) and an intergenic region (*IG*) at 2 and 5 d after germination (dag) as determined by chromatin immunoprecipitation (ChIP)-quantitative polymerase chain reaction (qPCR). Enrichment at *Ta3* at 2 dag in WT was set to 1. Histograms present mean percentages  $\pm$  SE for four biological replicates. WT vs *fas2-5* at the corresponding dag (Student's *t*-test): #,  $P < 0.1$ ; ##,  $P < 0.05$ . (b) H3K9me2 enrichment at 5 dag in WT and *h2a.w.6 h2a.w.7* mutants relative to H3 at 2 and 5 dag as determined by ChIP-qPCR at the same targets as in (a). *Ta3* for one biological replicate was set to 1. Histograms present mean percentages  $\pm$  SE for three biological replicates. (c) Model for local chromatin changes during chromocenter (CC) formation. Early after germination repetitive centromeric and pericentromeric sequences show low H3.1 and H2A.W occupancy but are already highly enriched in H3K9me2 and H1 compared to euchromatin. H3K9me2 and linker histone H1 enrichment therefore precedes organization into CC structures. During postgermination development, nucleosome occupancy increases modestly with concomitant changes in the H3.1 : H3.3 ratio at repetitive sequences; likely due to new H3.1 deposition during DNA replication, maybe involving H3.3 removal. Together with new H2A.W deposition, altered nucleosome stability in presence of H3.1 may promote CC formation and consolidate transcriptional silencing. Tightly coordinated replication-coupled histone assembly mediated by CAF-1 may favor H2A.W incorporation at specific sites as well as H3K9 methylation, possibly coupling post-translational modifications of non-nucleosomal histones with their subsequent deposition.

methylation. We confirmed this observation in the *fas1-4* allele (Fig. S4a).

In order to investigate if reduction in H3K9me2 levels indeed results from impaired DNA-synthesis dependent histone deposition, we first confirmed that the expression of the three major histone methyltransferase (HMT) genes *SUPPRESSOR OF VARIATION 3-9 HOMOLOGUE 4 (SUVH4)*, *SUVH5* and *SUVH6* (Ebbs, 2006) is not negatively affected in *fas2-5* mutant cotyledons (Fig S4b). Then, to exclude the hypothesis that defective CC organization perturbs HMT function and is causative for the reduction in H3K9me2, we assessed H3K9me2 levels in *h2a.w.6 h2a.w.7* double mutants with perturbed CC organization. Despite deficient CC organization at 5 dag in this mutant background (Fig. 4d), H3K9me2 levels are not significantly different between the *h2a.w* mutant and WT chromatin (Fig. 5b), excluding a role for nuclear organization of pericentromeric sequences *per se* in H3K9me2 deposition. Taken together, these results reveal a role for replication-coupled histone deposition in promoting H3K9 methylation at repetitive sequences in Arabidopsis.

## Discussion

Cytological studies have provided insights into the dynamics of chromatin organization during developmental phase transitions in plants. Chromocenter (CC) formation during the transition from heterotrophic to autotrophic growth in the young seedling that we have investigated here is thought to correlate with massive changes in gene expression occurring simultaneously with important alterations in nuclear architecture (Mathieu *et al.*, 2003; Douet *et al.*, 2008; Pontvianne *et al.*, 2010; van Zanten *et al.*, 2011). Preceding the progressive CC establishment in this developmental time window is nuclear expansion and chromatin decondensation of the highly condensed chromatin in the dry seed that are induced by imbibition (van Zanten *et al.*, 2011). Here we show that CC numbers and volume rise during seedling growth within the cotyledon tissue, correlating with simultaneous clustering of individual centromeric and pericentromeric repeats observed by FISH. These rearrangements occur with a well-defined pattern, therefore allowing the study of the consequences of altered histone deposition and modifications on naturally occurring changes in nuclear and chromatin organization. Indeed, our results imply tightly temporally controlled molecular mechanisms and establish a link between histone H3.1 and H2A.W enrichment and chromocenter formation during seedling development.

### Chromatin changes during CC formation

Given its involvement in chromatin fiber compaction (Fan *et al.*, 2005; Fyodorov *et al.*, 2018) and its enrichment at heterochromatin (Rutowicz *et al.*, 2015), the linker histone H1 is an interesting candidate to be involved in CC formation. Indeed, H1 loss is associated with chromatin relaxation and emerged as a common feature of epigenetic reprogramming in mammals (Hajkova *et al.*, 2008) and plants (She *et al.*, 2013). However,

despite dispersion of repeats in most nuclei at 2 dag, H1 is enriched at heterochromatic sequences compared to genes before their organization into CCs and does not increase further. H1 incorporation is therefore not sufficient for CC dynamics during cotyledon development. Instead, we find that core components of the nucleosomes dynamically change at repetitive sequences including the histone H3.1 and H2A.W.6 variants (Fig. 5c). Due to their influence on nucleosome stability (Jin & Felsenfeld, 2007) and chromatin fiber–fiber interaction (Yelagandula *et al.*, 2014), respectively, the structural characteristics of the nucleosome induced by these variants have the potential to promote CC formation and to reinforce transcriptional repression. The most striking difference at the nucleosomal level between dispersed and condensed repetitive sequences is the enrichment in the replicative histone H3.1. Several studies indicated that in Arabidopsis DNA replication is transiently activated at germination (Barroco *et al.*, 2005), in agreement with expression of genes encoding H3.1, and FAS1 and FAS2 (subunits of the CAF-1 complex) upon imbibition and germination. Cells proliferate in the cotyledon (Masubelele *et al.*, 2005) and then undergo endoreplication from 2 dag during tissue growth (Ramirez-Parra & Gutierrez, 2007), which is also evidenced by more elongated nuclei at day 5. Furthermore, ongoing DNA synthesis in cotyledons has been shown by incorporation in of the nucleotide analog 5-ethynyl-2'-deoxyuridine (EdU) 7-d-old seedlings (Jiang & Berger, 2017), together suggesting that DNA-synthesis-dependent deposition can explain the observed increased H3.1 occupancy at repetitive sequences at 5 dag. To explain the increase in H3.1 occupancy specifically at heterochromatin, we can envisage that after a genome-wide incorporation during S-phase, H3.1 is exchanged to H3.3 either in a transcription-dependent manner at the genic regions analyzed here or globally in euchromatin as described previously during the transition from cell proliferation to differentiation in the root (Otero *et al.*, 2016). Interestingly, most H3.1-encoding genes are not expressed in the dry seed (Kawakatsu *et al.*, 2017; Narsai *et al.*, 2017), in agreement with absence of replicative activity (Barroco *et al.*, 2005) pointing towards a peculiar H3.1 : H3.3 balance in the dry seed that might favor chromatin decondensation during germination. Furthermore, the resumption of replication activity after germination renders this developmental time window particularly suitable to decipher changes in chromatin and nuclear organization linked to DNA replication coupled histone deposition.

In support for an important function of the observed changes in the core histone composition in CC formation, the number of nuclei with fully formed CCs is significantly reduced in *fas1* and *fas2* mutants, but not in *hira* mutants deficient in H3.3 incorporation, echoing the requirement for CAF-1 in the formation of higher-order chromatin domains during early mouse development (Houlard *et al.*, 2006; Akiyama *et al.*, 2011). An effect of CAF-1 loss on the clustering of repetitive sequences into CCs is not restricted to cotyledons, but also has been observed in mature leaf tissue and roots (Kirik *et al.*, 2006; Schönrock *et al.*, 2006). In addition to H3.1, our data argue for a critical role of H2A.W incorporation in CC formation in the cotyledon likely due to the

intrinsic properties of H2A.W to promote long-range nucleosome–nucleosome interactions (Yelagandula *et al.*, 2014). In agreement, H2A.W.6 enrichment at repetitive sequences is dynamic between 2 and 5 dag and increases in a pattern reminiscent of H3.1. Furthermore, repeat clustering in cotyledons is strongly reduced in mutants lacking two of the three H2A.W-encoding genes, as observed in mature leaves (Yelagandula *et al.*, 2014). Although we find evidence that H3.1 and H2A.W.6 incorporation play a critical role in CC formation, we do not exclude the implication of other DNA- or chromatin-binding proteins (Jagannathan *et al.*, 2018).

### Impact of deficient replication-coupled histone deposition

Enrichment in histone H3 Lys-9 (H3K9) methylation is a characteristic feature of heterochromatin in plants and animals. Centromeric and pericentromeric domains in Arabidopsis cotyledons are strongly enriched in H3K9me2 even in the absence of CCs at 2 dag or in *h2a.w* mutants, similar to previous observations in leaf tissue (Yelagandula *et al.*, 2014). Consequently, CC formation is not a prerequisite for proper H3K9me2 methylation. Moreover, H3K9me2 loss in the triple methyltransferase mutant *suwh4 suwh5 suwh6* has only a subtle effect on CC organization (Stroud *et al.*, 2014). Hence, our results rather propose changes in the core histone variants as being critical for CC formation.

We find, however, that H3K9me2 levels during cotyledon development are reduced in the absence of functional CAF-1 complexes. Therefore, setting of H3K9me2 could be intimately linked to DNA replication. In mammals, CAF-1 was shown to play a central role in coordinating histone assembly with inheritance of histone modifications (Sarraf & Stancheva, 2004; Loyola *et al.*, 2009; Probst *et al.*, 2009). The same was observed for HETEROCHROMATIN PROTEIN 1 during heterochromatin replication (Quivy *et al.*, 2004). Furthermore, in plants, CAF-1 mediated H3.1 incorporation has recently been shown to be required for inheritance for H3K27me3 methylation, a process that involves the direct interaction between the largest subunit of the CAF-1 complex, FAS1 and Polycomb group proteins (Jiang & Berger, 2017). Our results now bring evidence that DNA-synthesis-dependent histone deposition is involved in the maintenance of H3K9me2. Several scenarios can be envisaged.

The uncoupling of DNA synthesis and chromatin assembly in the absence of CAF-1 increases the time between replication fork passage and chromatin assembly. Setting of H3K9me2 methylation is then delayed until compensatory complexes such as HIR and ALPHA THALASSEMIA-MENTAL RETARDATION X-LINKED (ATRX) (Nie *et al.*, 2014; Duc *et al.*, 2015, 2017) have restored nucleosome occupancy to allow for subsequent deposition of histone post-translational modifications.

Alternatively, similar to H3K27 monomethylation by ARABIDOPSIS THRITHORAX-RELATED PROTEIN 5 (ATXR5) and ATXR6 (Jacob *et al.*, 2014; Jiang & Berger, 2017), we can envisage replication-coupled modifications of histones bound to the CAF-1 complex. Such a mechanism has been suggested in mammals for the histone methyltransferase SETDB1 (Sarraf & Stancheva, 2004; Loyola *et al.*, 2009).

Finally, similarly to ATXR5 and ATXR6 (Jacob *et al.*, 2014), histone H3K9 methylases may exhibit some preference for the incorporated histone variants. We also found enhanced expression of the H3.3-like encoding genes *HTR6* and *HTR14* in *fas2-5* mutants. Although it is not clear yet how and where H3.6 and H3.14 are deposited, and whether these H3.3-like variants could be enriched at heterochromatin, it is intriguing to speculate that this incorporation might influence subsequent post-translational modifications. Indeed, the threonine 11 residue conserved in H3.1 and H3.3 is substituted by a histidine in H3.6 and H3.14 variants. This difference could impact histone methylation, as for example in mammals the histone methyltransferase G9a requires the heptapeptide at position 6–12 of the histone H3 tail (TARKSTG) as the minimal substrate (Rather *et al.*, 2008). Whether, H3K9me2 levels could be only transiently affected in CAF-1 mutants and correctly set later in development remains to be explored, but at least nucleosomal occupancy is only weakly affected in adult leaves of CAF-1 mutants, suggesting that compensatory mechanisms using alternative histone chaperone pathways are involved (Muñoz-Viana *et al.*, 2017).

As the first step in nucleosome assembly, deposition of the H3-H4 tetrameres has the potential to impact H2A-H2B deposition. Indeed, we observed that in the absence of CAF-1, H2A.W.6 occupancy is lower at heterochromatic regions such as *Ta3* and *CACTA*. Although we cannot exclude that this is reflecting reduced nucleosomal occupancy in *fas2* mutants, it is tempting to speculate that H2A.W deposition could be connected to CAF-1 activity during replication-coupled chromatin assembly. By contrast, we find no evidence that the altered chromatin composition in CAF-1 mutants negatively influences H1 deposition.

Taken together, we find that histone deposition and histone modifications function together in a highly dynamic manner to orchestrate CC formation. Proper chromatin assembly at the replication fork by CAF-1 likely facilitates *de novo* setting and propagation of H3K9me2 and may influence deposition of H2A.W. Our study shows that defective chromatin assembly in the absence of a functional CAF-1 complex impairs H3.1 deposition at repetitive elements, the coordinated setting of repressive chromatin marks and ultimately CC formation.

Conspicuous CC structures are a common feature of nuclear organization among several organisms. Our data further establish a correlation between CC formation and consolidation of transcriptional repression at heterochromatic repeats. Moreover, tight chromatin compaction may help in maintaining other heterochromatin features, such as late replication timing. Alternatively, it may contribute to minimizing recombination between sequences by restricting opportunities for interaction (Quivy *et al.*, 2004; Feng *et al.*, 2014; Grob *et al.*, 2014) and by preserving the full chromosome complement within the nucleus (Jagannathan *et al.*, 2018). As CCs potentially play an essential role in organizing euchromatic loops in the 3D space of the nucleus (Fransz *et al.*, 2002), it will be intriguing to explore how CC reorganization during seedling growth impacts the organization of euchromatin in nuclear space and how it

contributes to reprogram gene expression patterns during the transition from heterotrophic to autotrophic growth.

## Acknowledgements


We thank: C. Gutierrez for providing transgenic lines expressing H3.1-Myc and H3.3-Myc; Z. Lorkovic and F. Berger for the anti-H2A.W.6 antibody; K. Rutowicz and A. Jerzmanowski for the H1.1-GFP line; S. Tourmente for stimulating discussion; A. Eccher, M. Peyny, G. Pompeu, E. Vanrobays and in particular M. C. Espagnol for technical help; the Clermont-Ferrand Imagerie Confocale (CLIC) confocal imaging facility; and O. Mittelsten Scheid, J. Paszkowski and F. Barneche for critical reading. The work was supported by a doctoral stipend from the Region Auvergne, by a grant 'Aide Individuelle Jeunes Chercheurs' from the Fondation ARC and by the Agence National de Recherche ('Dynam'Her' ANR-11 JSV2 009 01, 'SINODYN' ANR-12 ISV6 0001, both to A.V.P.). This work was further supported by the Centre National de la Recherche Scientifique, the Institut National de la Santé et de la Recherche Médicale and the University Clermont Auvergne. The authors would like to acknowledge networking support from COST Action CA16212. The authors declare that they have no conflict of interest.

## Author contributions

A.V.P. and M.B. designed and planned the research; M.B., L.S., S.D., C.D., S.C., A.P., S.L.G. and A.V.P. performed experiments; M.B., L.S., S.D., C.D., S.C., A.P., S.L.G., C.T. and A.V.P. analyzed the data; and M.B. and A.V.P. wrote the manuscript.

## ORCID

Matthias Benoit  <http://orcid.org/0000-0002-3958-3173>

Aline V. Probst  <http://orcid.org/0000-0001-9534-8058>

## References

- Akiyama T, Suzuki O, Matsuda J, Aoki F. 2011. Dynamic replacement of histone H3 variants reprograms epigenetic marks in early mouse embryos. *PLoS Genetics* 7: e1002279.
- Almouzni G, Probst AV. 2011. Heterochromatin maintenance and establishment: lessons from the mouse pericentromere. *Nucleus* 2: 332–338.
- Barroco RM, Van Poucke K, Bergervoet JH, De Veylder L, Groot SP, Inze D, Engler G. 2005. The role of the cell cycle machinery in resumption of postembryonic development. *Plant Physiology* 137: 127–140.
- Benoit M, Layat E, Tourmente S, Probst AV. 2013. Heterochromatin dynamics during developmental transitions in Arabidopsis – a focus on ribosomal DNA loci. *Gene* 526: 39–45.
- Bourbousse C, Mestiri I, Zabulon G, Bourge M, Formigini F, Koini MA, Brown SC, Fransz P, Bowler C, Barneche F. 2015. Light signaling controls nuclear architecture reorganization during seedling establishment. *Proceedings of the National Academy of Sciences, USA* 112: E2836–E2844.
- Bowler C, Benvenuto G, Laflamme P, Molino D, Probst AV, Tariq M, Paszkowski J. 2004. Chromatin techniques for plant cells. *Plant Journal* 39: 776–789.
- Chodavarapu RK, Feng S, Bernatavichute YV, Chen PY, Stroud H, Yu Y, Hetzel JA, Kuo F, Kim J, Cokus SJ *et al.* 2010. Relationship between nucleosome positioning and DNA methylation. *Nature* 466: 388–392.
- Czechowski T, Stitt M, Altmann T, Udvardi MK, Scheible WR. 2005. Genome-wide identification and testing of superior reference genes for transcript normalization in Arabidopsis. *Plant Physiology* 139: 5–17.
- Desset S, Poulet A, Tatout C. 2018. Quantitative 3D analysis of nuclear morphology and heterochromatin organization from whole-mount plant tissue using Nucleus. In: Bemer M, Baroux C, eds. *Plant chromatin dynamics. Methods in molecular biology*. New York, NY, USA: Humana Press, 615–632.
- Douet J, Blanchard B, Cuvillier C, Tourmente S. 2008. Interplay of RNA Pol IV and ROS1 during post-embryonic 5S rDNA chromatin remodeling. *Plant and Cell Physiology* 49: 1783–1791.
- Duc C, Benoit M, Détourné G, Simon L, Poulet A, Jung M, Veluchamy A, Latrasse D, Le Goff S, Cotterell S *et al.* 2017. Arabidopsis ATRX modulates H3.3 occupancy and fine-tunes gene expression. *Plant Cell* 29: 1773–1793.
- Duc C, Benoit M, Le Goff S, Simon L, Poulet A, Cotterell S, Tatout C, Probst AV. 2015. The histone chaperone complex HIR maintains nucleosome occupancy and counterbalances impaired histone deposition in CAF-1 complex mutants. *Plant Journal* 81: 707–722.
- Ebbs ML. 2006. Locus-specific control of DNA methylation by the Arabidopsis SUVH5 histone methyltransferase. *Plant Cell* 18: 1166–1176.
- Fan Y, Nikitina T, Zhao J, Fleury TJ, Bhattacharyya R, Bouhassira EE, Stein A, Woodcock CL, Skoultschi AI. 2005. Histone H1 depletion in mammals alters global chromatin structure but causes specific changes in gene regulation. *Cell* 123: 1199–1212.
- Fang Y, Spector DL. 2005. Centromere positioning and dynamics in living Arabidopsis plants. *Molecular Biology of the Cell* 16: 5710–5718.
- Feng S, Cokus SJ, Schubert V, Zhai J, Pellegrini M, Jacobsen SE. 2014. Genome-wide Hi-C analyses in wild-type and mutants reveal high-resolution chromatin interactions in Arabidopsis. *Molecular Cell* 55: 694–707.
- Fransz P, de Jong JH, Lysak M, Castiglione MR, Schubert I. 2002. Interphase chromosomes in Arabidopsis are organized as well defined chromocenters from which euchromatin loops emanate. *Proceedings of the National Academy of Sciences, USA* 99: 14584–14589.
- Fransz P, ten Hoopen R, Tessoro F. 2006. Composition and formation of heterochromatin in *Arabidopsis thaliana*. *Chromosome Research* 14: 71–82.
- Fyodorov DV, Zhou B-R, Skoultschi AI, Bai Y. 2018. Emerging roles of linker histones in regulating chromatin structure and function. *Nature Reviews Molecular Cell Biology* 19: 192–206.
- Grob S, Schmid MW, Grossniklaus U. 2014. Hi-C analysis in *Arabidopsis* identifies the KNOT, a structure with similarities to the *flamenco* locus of *Drosophila*. *Molecular Cell* 55: 678–693.
- Hajkova P, Ancelin K, Waldmann T, Lacoste N, Lange UC, Cesari F, Lee C, Almouzni G, Schneider R, Surani MA. 2008. Chromatin dynamics during epigenetic reprogramming in the mouse germ line. *Nature* 452: 877–881.
- Houlard M, Berlivet S, Probst AV, Quivy J-PP, Héry P, Almouzni G, Gérard M. 2006. CAF-1 is essential for heterochromatin organization in pluripotent embryonic cells. *PLoS Genetics* 2: e181.
- Jacob Y, Bergamin E, Donoghue MTA, Mongeon V, LeBlanc C, Voigt P, Underwood CJ, Brunzelle JS, Michaels SD, Reinberg D *et al.* 2014. Selective methylation of histone H3 variant H3.1 regulates heterochromatin replication. *Science* 343: 1249–1253.
- Jagannathan M, Cummings R, Yamashita YM. 2018. A conserved function for pericentromeric satellite DNA. *eLife* 7: e34122.
- Jiang D, Berger F. 2017. DNA replication-coupled histone modification maintains Polycomb gene silencing in plants. *Science* 357: 1146–1149.
- Jin C, Felsenfeld G. 2007. Nucleosome stability mediated by histone variants H3.3 and H2A.Z. *Genes & Development* 21: 1519–1529.
- Jin C, Zang C, Wei G, Cui K, Peng W, Zhao K, Felsenfeld G. 2009. H3.3/H2A.Z double variant-containing nucleosomes mark 'nucleosome-free regions' of active promoters and other regulatory regions. *Nature Genetics* 41: 941–945.
- Kawakatsu T, Nery JR, Castanon R, Ecker JR. 2017. Dynamic DNA methylation reconfiguration during seed development and germination. *Genome Biology* 18: 171.

- Kaya H, Shibahara KI, Taoka KI, Iwabuchi M, Stillman B, Araki T. 2001. FASCIATA genes for chromatin assembly factor-1 in *Arabidopsis* maintain the cellular organization of apical meristems. *Cell* 104: 131–142.
- Kirik A, Pecinka A, Wendeler E, Reiss B. 2006. The chromatin assembly factor subunit FASCIATA1 is involved in homologous recombination in plants. *Plant Cell* 18: 2431–2442.
- Konieczny A, Voytas DF, Cummings MP, Ausubel FM. 1991. A superfamily of *Arabidopsis thaliana* retrotransposons. *Genetics* 127: 801–809.
- Loyola A, Bonaldi T, Roche D, Imhof A, Almouzni G. 2006. PTMs on H3 variants before chromatin assembly potentiate their final epigenetic state. *Molecular Cell* 24: 309–316.
- Loyola A, Tagami H, Bonaldi T, Roche D, Quivy JP, Imhof A, Nakatani Y, Dent SYR, Almouzni G. 2009. The HP1alpha – CAF1 – SetDB1-containing complex provides H3K9me1 for Suv39-mediated K9me3 in pericentric heterochromatin. *EMBO Reports* 10: 769–775.
- Martens JH, O'Sullivan RJ, Braunschweig U, Opravil S, Radolf M, Steinlein P, Jenuwein T. 2005. The profile of repeat-associated histone lysine methylation states in the mouse epigenome. *EMBO Journal* 24: 800–812.
- Masubelele NH, Dewitte W, Menges M, Maughan S, Collins C, Huntley R, Nieuwland J, Scofield S, Murray JA. 2005. D-type cyclins activate division in the root apex to promote seed germination in *Arabidopsis*. *Proceedings of the National Academy of Sciences, USA* 102: 15694–15699.
- Mathieu O, Jasencakova Z, Vaillant I, Gendrel AV, Colot V, Schubert I, Tourmente S. 2003. Changes in 5S rDNA chromatin organization and transcription during heterochromatin establishment in *Arabidopsis*. *Plant Cell* 15: 2929–2939.
- Mathieu O, Probst AV, Paszkowski J. 2005. Distinct regulation of histone H3 methylation at lysines 27 and 9 by CpG methylation in *Arabidopsis*. *EMBO Journal* 24: 2783–2791.
- May BP, Lippman ZB, Fang Y, Spector DL, Martienssen RA. 2005. Differential regulation of strand-specific transcripts from *Arabidopsis* centromeric satellite repeats. *PLoS Genetics* 1: e79.
- Mayer R, Brero A, von Hase J, Schroeder T, Cremer T, Dietzel S. 2005. Common themes and cell type specific variations of higher order chromatin arrangements in the mouse. *BMC Cell Biology* 6: 44.
- Muñoz-Viana R, Wildhaber T, Trejo-Arellano MS, Mozgová I, Hennig L. 2017. *Arabidopsis* Chromatin Assembly Factor 1 is required for occupancy and position of a subset of nucleosomes. *Plant Journal* 38: 42–49.
- Narsai R, Gouil Q, Secco D, Srivastava A, Karpievitch YV, Liew LC, Lister R, Lewsey MG, Whelan J. 2017. Extensive transcriptomic and epigenomic remodelling occurs during *Arabidopsis thaliana* germination. *Genome Biology* 18: 172.
- Nie X, Wang H, Li J, Holec S, Berger F. 2014. The HIRA complex that deposits the histone H3.3 is conserved in *Arabidopsis* and facilitates transcriptional dynamics. *Biology Open* 3: 794–802.
- Otero S, Desvoyes B, Peiró R, Gutierrez C. 2016. Histone H3 dynamics reveal domains with distinct proliferation potential in the *Arabidopsis* root. *Plant Cell* 28: 1361–1371.
- Pavet V, Quintero C, Cecchini NM, Rosa AL, Alvarez ME. 2006. *Arabidopsis* displays centromeric DNA hypomethylation and cytological alterations of heterochromatin upon attack by *Pseudomonas syringae*. *Molecular Plant–Microbe Interactions* 19: 577–587.
- Pecinka A, Dinh HQ, Baubec T, Rosa M, Lettner N, Mittelsten Scheid O. 2010. Epigenetic regulation of repetitive elements is attenuated by prolonged heat stress in *Arabidopsis*. *Plant Cell* 22: 3118–3129.
- Pontvianne F, Abou-Ellail M, Douet J, Comella P, Matia I, Chandrasekhara C, Debures A, Blevins T, Cooke R, Medina FJ *et al.* 2010. Nucleolin is required for DNA methylation state and the expression of rRNA gene variants in *Arabidopsis thaliana*. *PLoS Genetics* 6: e1001225.
- Poulet A, Arganda-Carreras I, Legland D, Probst AV, Andrey P, Tatout C. 2015. NucleusJ: an ImageJ plugin for quantifying 3D images of interphase nuclei. *Bioinformatics* 31: 1144–1146.
- Poulet A, Duc C, Voisin M, Desset S, Tutois S, Vanrobays E, Benoit M, Evans DE, Probst AV, Tatout C. 2017. The LINC complex contributes to heterochromatin organisation and transcriptional gene silencing in plants. *Journal of Cell Science* 130: 590–601.
- Probst AV, Dunleavy E, Almouzni G. 2009. Epigenetic inheritance during the cell cycle. *Nature reviews Molecular Cell biology* 10: 192–206.
- Probst AV, Fransz PF, Paszkowski J, Mittelsten Scheid O. 2003. Two means of transcriptional reactivation within heterochromatin. *Plant Journal* 33: 743–749.
- Probst AV, Mittelsten Scheid O. 2015. Stress-induced structural changes in plant chromatin. *Current Opinion in Plant Biology* 27: 8–16.
- Quivy JP, Roche D, Kirschner D, Tagami H, Nakatani Y, Almouzni G. 2004. A CAF-1 dependent pool of HP1 during heterochromatin duplication. *EMBO Journal* 23: 3516–3526.
- Ramirez-Parra E, Gutierrez C. 2007. E2F regulates FASCIATA1, a chromatin assembly gene whose loss switches on the endocycle and activates gene expression by changing the epigenetic status. *Plant Physiology* 144: 105–120.
- Rathert P, Dhayalan A, Murakami M, Zhang X, Tamas R, Jurkowska R, Komatsu Y, Shinkai Y, Cheng X, Jeltsch A. 2008. Protein lysine methyltransferase G9a acts on non-histone targets. *Nature Chemical Biology* 4: 344–346.
- Rutowicz K, Puzio M, Halibart-Puzio J, Lirski M, Kroteń MA, Kotliński M, Knížewski Ł, Lange B, Muszewska A, Śniegowska-Świerk K *et al.* 2015. A specialized histone H1 variant is required for adaptive responses to complex abiotic stress and related DNA methylation in *Arabidopsis*. *Plant Physiology* 169: 2080–2101.
- Sarraf SA, Stancheva I. 2004. Methyl-CpG binding protein MBD1 couples histone H3 methylation at lysine 9 by SETDB1 to DNA replication and chromatin assembly. *Molecular Cell* 15: 595–605.
- Schönrock N, Exner V, Probst AV, Gruissem W, Hennig L. 2006. Functional genomic analysis of CAF-1 mutants in *Arabidopsis thaliana*. *Journal of Biological Chemistry* 281: 9560–9568.
- She W, Baroux C. 2015. Chromatin dynamics in pollen mother cells underpin a common scenario at the somatic-to-reproductive fate transition of both the male and female lineages in *Arabidopsis*. *Frontiers in Plant Science* 6: 294.
- She W, Grimaneli D, Rutowicz K, Whitehead MWJ, Puzio M, Kotlinski M, Jerzmanowski A, Baroux C. 2013. Chromatin reprogramming during the somatic-to-reproductive cell fate transition in plants. *Development* 140: 4008–4019.
- Shu H, Nakamura M, Siretskiy A, Borghi L, Moraes I, Wildhaber T, Gruissem W, Hennig L. 2014. *Arabidopsis* replacement histone variant H3.3 occupies promoters of regulated genes. *Genome Biology* 15: R62.
- Shu H, Wildhaber T, Siretskiy A, Gruissem W, Hennig L. 2012. Distinct modes of DNA accessibility in plant chromatin. *Nature Communications* 3: 1281.
- Simon L, Voisin M, Tatout C, Probst AV. 2015. Structure and function of centromeric and pericentromeric heterochromatin in *Arabidopsis thaliana*. *Frontiers in Plant Science* 6: 1049.
- Smith S, Stillman B. 1991. Stepwise assembly of chromatin during DNA replication *in vitro*. *EMBO Journal* 10: 971–980.
- Snoek BL, Pavlova P, Tessadori F, Peeters AJM, Bourbousse C, Barneche F, de Jong JH, Fransz PF, van Zanten M. 2017. Genetic dissection of morphometric traits reveals that Phytochrome B affects nucleus size and heterochromatin organization in *Arabidopsis thaliana*. *G3: Genes, Genomes, Genetics* 7: 2519–2531.
- Steimer A, Amedeo P, Afsar K, Fransz P, Mittelsten Scheid O, Paszkowski J. 2000. Endogenous targets of transcriptional gene silencing in *Arabidopsis*. *Plant Cell* 12: 1165–1178.
- Stroud H, Do T, Du J, Zhong X, Feng S, Johnson L, Patel DJ, Jacobsen SE. 2014. Non-CG methylation patterns shape the epigenetic landscape in *Arabidopsis*. *Nature Structural & Molecular Biology* 21: 64–72.
- Stroud H, Otero S, Desvoyes B, Ramirez-Parra E, Jacobsen SE, Gutierrez C. 2012. Genome-wide analysis of histone H3.1 and H3.3 variants in *Arabidopsis thaliana*. *Proceedings of the National Academy of Sciences, USA* 109: 5370–5375.
- Sura W, Kabza M, Karlowski WM, Bieluszewski T, Kuś-Słowinska M, Pawelozek Ł, Sadowski J, Ziolkowski PA. 2017. Dual role of the histone variant H2A.Z in transcriptional regulation of stress-response genes. *Plant Cell* 29: 791–807.
- Tessadori F, Chupeau MC, Chupeau Y, Knip M, Germann S, van Driel R, Fransz P, Gaudin V. 2007a. Large-scale dissociation and sequential reassembly

- of pericentric heterochromatin in dedifferentiated *Arabidopsis* cells. *Journal of Cell Science* 120: 1200–1208.
- Tessadori F, Schulkes RK, van Driel R, Fransz P. 2007b. Light-regulated large-scale reorganization of chromatin during the floral transition in *Arabidopsis*. *Plant Journal* 50: 848–857.
- Thakar A, Gupta P, Ishibashi T, Finn R, Silva-Moreno B, Uchiyama S, Fukui K, Tomschik M, Ausio J, Zlatanova J. 2009. H2A.Z and H3.3 histone variants affect nucleosome structure: biochemical and biophysical studies. *Biochemistry* 48: 10852–10857.
- Wollmann H, Holec S, Alden K, Clarke N, Jacques P, Berger F. 2012. Dynamic deposition of histone variant h3.3 accompanies developmental remodeling of the *Arabidopsis* transcriptome. *PLoS Genetics* 8: e1002658.
- Wollmann H, Stroud H, Yelagandula R, Tarutani Y, Jiang D, Jing L, Jamge B, Takeuchi H, Holec S, Nie X *et al.* 2017. The histone H3 variant H3.3 regulates gene body DNA methylation in *Arabidopsis thaliana*. *Genome Biology* 18: 94.
- Yelagandula R, Stroud H, Holec S, Zhou K, Feng S, Zhong X, Muthurajan UM, Nie X, Kawashima T, Groth M *et al.* 2014. The histone variant H2A.W defines heterochromatin and promotes chromatin condensation in *Arabidopsis*. *Cell* 158: 98–109.
- van Zanten M, Koini MA, Geyer R, Liu Y, Brambilla V, Bartels D, Koornneef M, Fransz P, Soppe WJ. 2011. Seed maturation in *Arabidopsis thaliana* is characterized by nuclear size reduction and increased chromatin condensation. *Proceedings of the National Academy of Sciences, USA* 108: 20219–20224.
- van Zanten M, Tessadori F, Peeters AJ, Fransz P. 2012. Shedding light on large-scale chromatin reorganization in *Arabidopsis thaliana*. *Molecular Plant* 5: 583–590.

## Supporting Information

Additional Supporting Information may be found online in the Supporting Information section at the end of the article.

**Fig. S1** H3.1 expression is dynamic during germination and post-germination development.

**Fig. S2** Nuclear H3.1 pools are reduced in CHROMATIN ASSEMBLY FACTOR 1 mutants and chromocenter clustering is impaired in *fas1*, but not in *hira* mutants.

**Fig. S3** Expression dynamics of histone variants-encoding genes in WT and *fas2-5* mutants and confirmation of histone H1 enrichment patterns along heterochromatin and genes.

**Fig. S4** H3K9me2 levels in *fas1-4* cotyledons and expression dynamics of the histone methyltransferase genes *SUPPRESSOR OF VARIATION 3-9 HOMOLOGUE 4 (SUVH4)*, *SUVH5* and *SUVH6* in WT and *fas2-5* mutants.

**Table S1** List of primers used in this study

**Methods S1** Western blot analysis of nuclear histones.

Please note: Wiley Blackwell are not responsible for the content or functionality of any Supporting Information supplied by the authors. Any queries (other than missing material) should be directed to the *New Phytologist* Central Office.



## About New Phytologist

- *New Phytologist* is an electronic (online-only) journal owned by the New Phytologist Trust, a **not-for-profit organization** dedicated to the promotion of plant science, facilitating projects from symposia to free access for our Tansley reviews and Tansley insights.
- Regular papers, Letters, Research reviews, Rapid reports and both Modelling/Theory and Methods papers are encouraged. We are committed to rapid processing, from online submission through to publication 'as ready' via *Early View* – our average time to decision is <26 days. There are **no page or colour charges** and a PDF version will be provided for each article.
- The journal is available online at Wiley Online Library. Visit **www.newphytologist.com** to search the articles and register for table of contents email alerts.
- If you have any questions, do get in touch with Central Office (np-centraloffice@lancaster.ac.uk) or, if it is more convenient, our USA Office (np-usaoffice@lancaster.ac.uk)
- For submission instructions, subscription and all the latest information visit **www.newphytologist.com**